



Treball Final de Grau

Intercalation of small molecules into metal halides
Intercalació de petites molècules dins d'halurs metàl·lics

Judit Vives Caldas

June 2021



UNIVERSITAT DE
BARCELONA

B:KC Barcelona
Knowledge
Campus
Campus d'Excel·lència Internacional

Aquesta obra esta subjecta a la llicència de:
Reconeixement–NoComercial–SenseObraDerivada



<http://creativecommons.org/licenses/by-nc-nd/3.0/es/>

El camí al progrés no és ni ràpid ni fàcil.

Marie Curie

Primer de tot vull donar les gràcies a totes les amistats que he fet durant aquests quatre anys, per fer les hores d'estudi més suportables. També vull donar les gràcies a la meva família per tot el suport que m'han donat al llarg de tota la carrera, sense ells no hauria sigut possible. Per últim, vull donar les gràcies al meu tutor, Dr. Eliseo Ruiz per haver-me guiat al llarg d'aquesta experiència, i el Jose Mauricio per haver-me dedicat tant temps a ajudar-me a expandir els mes coneixements, sobretot les llargues hores a l'AFM.

REPORT

CONTENTS

1. SUMMARY	3
2. RESUM	5
3. INTRODUCTION	7
3.1. Layered materials	7
3.2. Intercalation process	11
3.3. Intercalation methods	13
3.3.1. Direct reactions	13
3.3.2. Ion-exchange reactions	14
3.3.3. Electrointercalation reactions	15
3.3.4. Rate Enhancement methods	15
3.4. Intercalated 2D compounds	15
3.4.1. Transitional metal dichalcogenides	17
3.4.2. Transition metal oxyhalides	18
3.4.3. Metal trichalcogenidophosphates	18
3.4.4. Metal oxides	19
3.4.5. Graphite intercalation compounds	19
3.4.6. MXenes	21
3.5 Intercalated ionic rock-salts structures	21
4. OBJECTIVES	26
5. EXPERIMENTAL SECTION	27
5.1. Experimental procedure	27
5.1.1. Exfoliation method and preparation of the sample for the AFM	29
5.1.1.1 Other tests performed	30
5.2. Powder X-ray diffraction	30
5.3. Atomic force microscopy	31

6. RESULTS AND DISCUSSION	33
6.1. Intercalation of Br ₂ in NaCl-type metal halides	33
6.2. X-ray Diffraction results	34
6.3. Crystallinity	35
6.4. Exfoliation properties	35
10. CONCLUSIONS	39
11. REFERENCES AND NOTES	41
12. ACRONYMS	43
APPENDICES	45
Appendix 1: Times of each intercalation process	47
Appendix 2: X-Ray powder diffractograms of CsF	49
Appendix 3: X-ray single-crystal results	51
Appendix 4: Graphics obtained with NanoScope Analysis program	53

1. SUMMARY

The layered materials are an extended family of solid crystals made up of a single or few thin layers of atoms stacked together by weak interlayer forces, usually *van der Waals* forces. These materials are liable to undergo intercalation reactions adopting unique properties and structural characteristics. A wide range of applications are known such as electrocatalysis devices, heterogeneous catalysis, supercapacitors and for energy storage.

The principal objective of this research was to obtain ionic layered systems based on metal halides that present a 3D structure with NaCl-lattice type, using bromine as intercalation guest. Specifically, NaCl, KCl, NaF, KF, AgF and CsF have been employed because of their favorable interactions and unit cell size. Intercalated samples were synthesized to study the bromine insertion process by means of powder X-ray diffraction.

Finally, it was studied the exfoliation properties with AFM, focusing on the intercalated cesium fluoride systems. The theoretical studies previously done indicates us these compounds present certain facilities to be exfoliated, fact that was investigated with the obtained AFM images.

Keywords: layered materials, *van der Waals*, ionic layered systems, exfoliation properties, AFM.

2. RESUM

Els materials 2D són una extensa família de cristalls sòlids que estan compostos d'una o varies capes molt fines unides entre elles per forces intermoleculares dèbils, normalment, forces de *van der Waals*. Aquests materials són susceptibles a presentar fàcilment reaccions d'intercalació adoptant unes propietats i característiques estructurals úniques, tenint així un ventall ampli d'aplicacions com ara en l'electrocatalisi, catalisi heterogènia, supercondensadors i en l'emmagatzematge d'energia.

L'objectiu principal d'aquest treball era obtenir sistemes iònics 2D a partir d'halurs metàl·lics que presenten una estructura 3D de tipus NaCl, utilitzant el brom com a molècula intercalant. Concretament s'ha treballat amb NaCl, KCl, NaF, KF, AgF i CsF per les seves favorables interaccions i mida de cel·la. Les mostres intercalades van ser sintetitzades per estudiar el procés d'inserció de les molècules de Br₂ mitjançant difracció de raig X en pols.

Finalment, es va estudiar la seva capacitat de ser exfoliats amb l'AFM, concretament amb els sistemes intercalats de fluorur de cesi. Els estudis teòrics fets prèviament ens indicaven que aquests compostos presenten certa facilitat a ser exfoliats, fet que es va investigar amb les imatges obtingudes del microscopi atòmic.

Paraules clau: materials 2D, *van der Waals*, sistemes iònics 2D, exfoliats, microscopi atòmic.

3. INTRODUCTION

3.1 LAYERED MATERIALS

The solid materials can be categorized into two types relay on the composition and crystal structure, layered and non-layer structured materials¹. In this research we will focus on the first one. Layered materials are composed of planes of atoms placed together by interplanar forces which are weaker than intraplanar bonds.

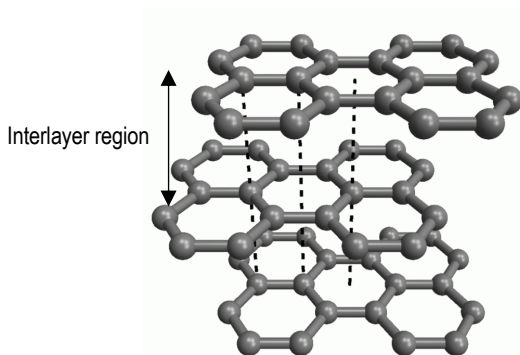


Figure 1: crystal structure of graphite²

There are three types of two-dimensional layered materials depend on the interplanar forces³. The first type of 2D materials present atomically thin sheets hold together by *van der Waals forces* where the magnitude of this interactions depends on the atomic weight of the involved materials and the configuration of the stacking⁴. The graphite and boron nitride belong to this group. Graphite is the most typical example of layered materials where layers of graphene pile together to form graphite crystal. Furthermore, there are layered materials composed of various planes held together by *van der Waals forces* such as transitional metal dichalcogenides and metal oxyhalides. On the contrary of these two types of layered materials, the third type is made up of charged layers connected by interlayer ionic forces. Examples are silicate clays and layered double hydroxides that present a rigid structure to interlayer distortion or expansion. Obviously, there is

an extended field which is not possible to cover in a single research and the table 1 tries to give a general outline of these large family^{1,3,5}.

Moreover, each layer has a complete chemical structure which makes relatively stable every single layer. In 2004³, with the discovery of the graphene began a new era in 2D materials with the study of an extended variety of inorganic, organic and hybrids compounds. Initially, the layered materials were considered to intercalated mainly molecules or also layers to generate hybrid materials combining the physical properties of the two compounds. However, it was found an extended variety of 2D materials applications in many areas of technology¹. Many researchers have focused on the two-dimensional materials in view of the novel properties that can be achieved. Owing to the weak forces layered materials are suitable through direct exfoliation or by the insertion guest species in the original lattice facilitating the exfoliation process⁵. Thus, such new 2D systems suffers a variation of their physical and chemical properties in comparison with the corresponding bulk structure opening a wide range of new properties.

Table 1: Classification of layered materials^{1,3,5}

Lattice Type	Illustrative examples
Elemental	Graphite Black-Phosphorus (BP) Hexagonal Boron Nitride (h-BN) Graphitic Carbon Nitride (g-C ₃ N ₄)
Metal chalcogenides	MX ₂ (M= Ti, Zr, Hf, V, Nb, Ta, Mo, W; X= S, Se) AMS ₂ (M= Ti, V, Cr, Mn, Fe, Co, Ni; A= group 1)
Metal trichalcogenidophosphates	MPX ₃ (M= Mg, V, Mn, Fe, Co, Ni, Zn, Cd, In; X= S, Se)
III-VI layered semiconductors	MX (M= Ga, In; X= S, Se, Te)
Metal oxides	M _x O _y (MoO ₃ , Mo ₁₈ O ₅₂ , V ₂ O ₅ , LiNbO ₂ , Li _x V ₃ O ₈) MOXO ₄ (M= Ti, V, Cr, Fe; X= P, As)
Transition metal oxyhalides	MOX (M= Ti, V, Cr, Fe; X= Br, Cl) Titanates K[Ca ₂ Na _{n-3} Nb ₂ O _{2n+1}]; 3 ≤ n ≤ 7 Niobates (K ₂ Ti ₄ O ₉)
Metal halides	MX _n (M= metal; X= F, Cl, Br, I)

	α -RuCl ₃
	β -ZrNCl
Metal phosphates and phosphonates	Zr(RPO ₃) ₂ , Zr(ROPO ₃) ₂ (R= Ph, Me, Et, etc.)
Silicates and hydroxides (Clay minerals)	Karolinitides [Al ₄ Si ₄ O ₁₀ (OH) ₈] Montmorillonite {Ca _{0.35} [Mg _{0.7} Al _{3.3}](Si ₈)O ₂₀ (OH) ₄ }
Layered double hydroxides (LDHs)	[M ^{z+} _{1-x} M ³⁺ _x (OH) ₂] ^{m+} [A ⁿ⁻] _{m/n} ·yH ₂ O (M ^{z+} = Mg ²⁺ , Zn ²⁺ , Ni ²⁺ , etc.; Z=2; M ³⁺ = Al ³⁺ , Ga ³⁺ , Fe ³⁺ , etc.; m=x; A ⁿ⁻ = CO ₃ ²⁻ , Cl ⁻ , SO ₄ ²⁻ , RCO ₂ ⁻)
Metal carbides (MXenes)	M _{n+1} AX _n (n = 1, 2, 3; M=Ti, V, Cr, Nb, etc.; A= Al, Si, Sn, In, etc.)
2D Metal-organic Frameworks (MOFs)	Zn-TCPP
2D perovskites	(A) ₂ (B) _{n-1} Pb _n X _{3n+1} (X= halide ion; B= FA or MA; A= long-chain cation)
2D zeolites	M _{2/n} O·Al ₂ O ₃ ·xSiO ₂ ·xH ₂ O (n= valency of cation)

2D inorganic compounds are defined as solid crystals made up of a single or few layers of atoms with 1-10 Å thickness and lateral dimensions of microns. Layered materials are a large family that include transitional metal dichalcogenides (TMDs), monochalcogenides, metal oxides, black phosphorus (BP) and hexagonal boron nitride (h-BN), among others as shown on the previous table^{1,3,5}. These layered materials present unique electronic, structural, mechanical, optical and magnetic properties. The main properties in this kind of systems are optoelectronic and photoelectronic properties^{1,6,7}(see Figure 2). What is more, the synthesis of these type of materials provided a new scope of smart technology¹.

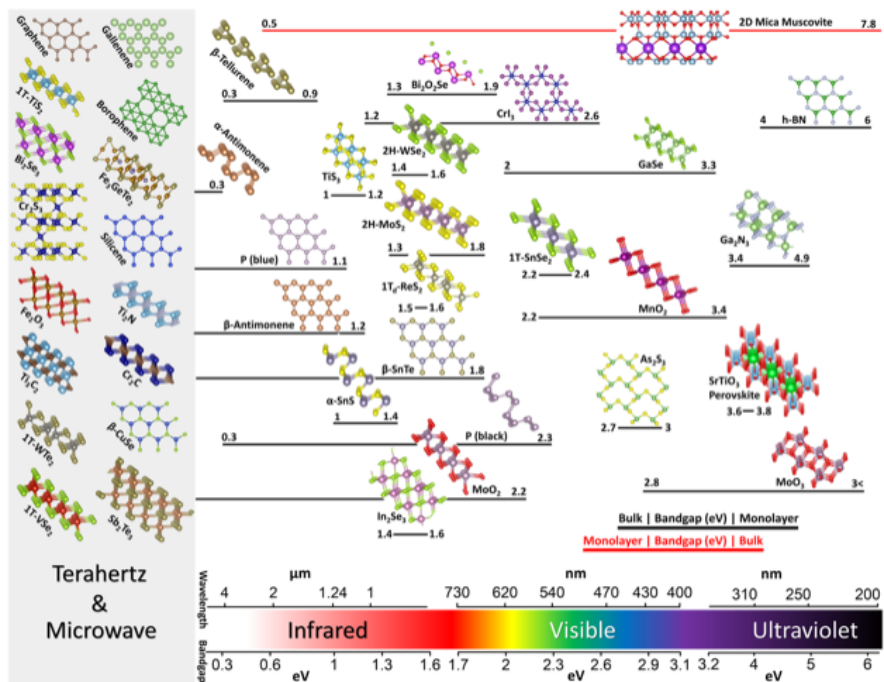


Figure 2: general illustration of the extended family of Two-Dimensional materials⁸

Taking black Phosphorous as an example, since his exfoliation a lot of studies emerge³. Due to the different arrangement of the atoms, there are various phosphorous allotropes and BP is the most important one because of the structural stability. A BP monolayer is made up of a puckered honeycomb structure and the P intralayer are connected by covalent bonds and the monolayers phosphorus are held together by *van der Waals forces* to form the BP bulk with semiconductor, electron and optoelectronic properties. Moreover, 2D BP have more advantages than de black phosphorus bulk because the layered structure has an extended area of applications such as photodetector, catalysis, batteries, supercapacitors and biomedicine. Although, it is the most difficult allotrope to synthetize because requires a high-pressure environment. As indicated on the table 1, graphite and BP present many similar features, but an important difference was found³. The plane of monolayer BP presents in-plane anisotropy, and on the contrary, the monolayer graphite is smooth^{1,3,9}.



Figure 3: Layered BP³

Regarding to 2D TMDs have a sphere of potential applications such as nanoelectronics, photodetectors, quantum devices, optical and catalysis. The ion transport in the most common analogous of graphite, MoS₂ unlock new opportunities in the area of neuromorphic computing⁹⁻¹¹. Currently, it has been working on the development of new synthetic methods to control the crystalline quality, defects and crystal phases to be commercialized. In comparison with graphene such systems have more stable electronic properties, and they behave as semiconductor. Thus, they are replacing graphene in many optoelectronic devices¹².

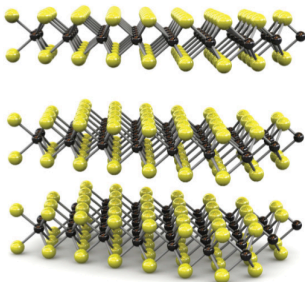


Figure 4: Schematic representation of the structure of a TMD material with general formula MX₂ where metallic atoms (M) are shown in black and chalcogens (X) in yellow spheres¹⁰

As highlighted in this chapter, the scope of 2D materials and their applications are in full growth and diversifying. The next step is to find out if the theoretical predictions can be experimentally demonstrated and guide experiments in the research of new functionalities and improve nanomaterial properties and applications¹³.

3.2 INTERCALATION PROCESS

Nowadays, the term intercalation on chemistry is used to describe the reversible insertion of mobile guest species such as atoms, molecules or ions into a crystalline host lattice. Guest materials include metal ions, organic and organometallic molecules. Intercalation reactions with layered lattices have been deeply studied due to the structural flexibility and facility to adapt to

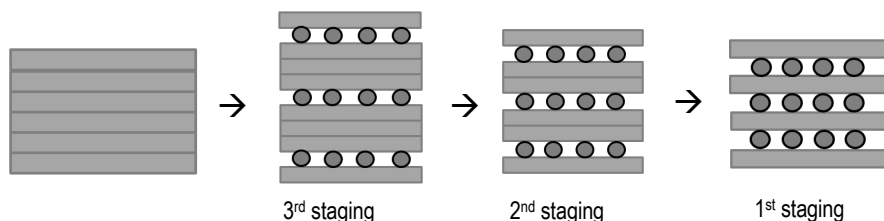
the geometry of the inserted guest by modification the interlayer separation¹⁴. These reactions typically occur around room temperature, but a wide range of host lattice needs a low-temperature environment to undergo the intercalation process.



Equation 1: general reaction for intercalation process⁵

Intercalation reactions catch the attention of organic, inorganic and physical chemistry⁵. The most interesting fact of this reactions is that during the intercalation process the host and guest experience perturbations in their geometrical, chemical and electronic environment. The principal geometrical changes through the guest insertion are the modification of the interlayer spacing, the stacking mode of the layers and the formation of the intermediate phase. As previously commented, intercalation reactions are usually reversible, and they may be considered as topochemical processes. In other words, it is a chemical reaction that occurs at the boundary of solid phases. Structurally, there are three types of host, framework (3D), layer (2D) and lineal (1D)⁵. Moreover, layer phases tend to have strong intralayer bonding and weak interlayer interactions, and each layer could be neutral or charged. On the first case, the interactions between layers often describes as *van der Waals* forces, but in the charged layered systems electrostatic forces appears^{3,5}.

Before talking about the inorganic intercalation compounds it is important to know some aspects about the kinetics and mechanisms of intercalation⁵. It has been possible to prepare a 2D metal nanostructure stables kinetically but thermodynamically have a tendency to adopt an isotropic shape to reduce the relation surface-volume if enough energy is given. Because of this, it has been developed new alternatives^{1,3,5}. In this type of reactions bonds are usually broken in the host lattice and appears new interactions between the host and the inserted guest. There is a phenomenon called staging and the order of the staging is given by the number of layers between successive sheets. This means it could be prepared intercalation compounds with specific stoichiometry as shown on the next chapter with cesium fluoride. Not long ago it was not clear if the origin of this phenomenon was for a structural or electronic reason, but it is known the size of the guest and the concentration of the species affect at the degree staging^{4,5}.

Figure 5: Levels of the phenomenon staging⁴

Intercalation compounds are produced by the insertion of the atomic or molecular species into a host lattice and many common solid materials present this property. Inorganic materials with layered structure usually undergo an expansion or swelling in front of the intercalation of guest species and due to the weakness of the interlayer interactions, the exfoliation of 2D layers is possible⁵.

3.3. INTERCALATION METHODS

At the present times many synthetic methods are known⁵. The advances in the synthesis of the intercalation systems has allowed to discover a lot of new intercalation compounds^{1,15}. The intercalation process is quite useful to exfoliate such materials to obtain nanoscopic 2D layers. In this section it will be exposed these new methods that provide a several advances on the intercalation chemistry. The reactions that lead to intercalated substances are considered as reversible topotactic solid-state reactions¹⁴.

3.3.1. Direct reactions

The direct reaction is the method used in the experimental part of this investigation and the most common technique. The following diagram illustrates the general procedure.

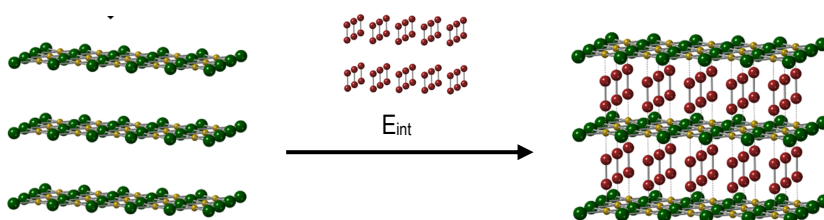


Figure 6: General representation of the intercalation reaction

It is important to highlight the products of the intercalation reactions tend to be insoluble. Consequently, they cannot be purified or separated of secondary products. Therefore, the synthetic strategy must be clean⁵.

Direct reactions are a good choice of general method for intercalate alkali metals and less reactive post transitional metals. Although, it is found the most reactive alkali metals products presents thermal instability and tend to give non-intercalation compounds⁵. Furthermore, in order to achieve the correct progress of the reaction, the intercalation reagent had to be suitable inside of the reduction side of the host lattice. Usually toluene, acetonitrile, dimethoxyethane and dimethylformamide seems to be a successful option for a wide range of systems. Besides, a highly polar solvents used to co-intercalate.

Table 2: Examples of intercalation compounds prepared by direct reaction⁵

Reactants	Products	Reaction conditions
$0.25 [\text{Co}(\text{Cp})_2] + \text{VSe}_2 \rightarrow$	$\text{VSe}_2[\text{Co}(\text{Cp})_2]_{0.25}$	130°C
$\text{K}_{(\text{metal})} + \text{C} (\text{graphite}) \rightarrow$	C_8K	200°C
$\text{LiBu}^n + \text{V}_6\text{O}_{13} \rightarrow$	$\text{Li}_x\text{V}_6\text{O}_{13}$	Hexane, 20°C
$\text{HCl/Zn} + \text{WO}_3 \rightarrow$	H_xWO_3	H_2O , 25°C
$\text{OsF}_6 + \text{C}(\text{graphite}) \rightarrow$	$\text{C}_8(\text{OsF})_6$	20°C
$\text{V}_2\text{O}_5 + x\text{LiI} \rightarrow$	$\text{Li}_x\text{V}_2\text{O}_5$	-
$\text{CsF} + \text{Br}_2 \rightarrow$	$\text{CsF} \cdot \text{Br}_2$	75°C

3.3.2. Ion-exchange reactions

Pre-intercalating and exchange the cation results to be a good alternative of direct reactions⁵. When an intercalation compound has been obtained, the intercalation guest could be replaced for another guest ion. These types of reactions, called ion-exchange are useful for alkali metal. What is more, intercalation reactions of zeolites, pyrochlores, silicates and clay minerals progress by ion-exchange reactions.

Table 3: Examples of intercalation compounds prepared by ion-exchange⁵

Reactants	Products	Reaction conditions
$\text{Na}_x\text{TiS}_2 + \text{LiPF}_6 \rightarrow$	Li_xTiS_2	Dioxolane, 25°C
$\text{Na}_{0.33}(\text{H}_2\text{O})_{0.66}\text{TaS}_2 + [\text{Co}(\text{Cp})_2]^+\text{I}^- \rightarrow$	$\text{TaS}_2[\text{Co}(\text{Cp})_2]_{0.2}$	Metanol, 25°C
$\text{Na}_{0.5}(\text{H}_2\text{O})_y\text{MoO}_3 + 0.25\text{Mg}^{2+} \rightarrow$	$\text{Mg}_{0.25}(\text{H}_2\text{O})_y\text{MoO}_3$	H_2O , 1M in Mg^{2+}

3.3.3. Electrointercalation reactions

In case the stoichiometry had to be controlled, electrointercalation methods are the best option where the host lattice performs as the cathode of the electrochemical cell. Nonetheless, electrointercalation methods are not the best choice for insert neutral guests or for insulating hosts. In contrast to conventional techniques, electrolysis methods provide a high rate of reactions at room temperature and detailed thermodynamic measurements to study the grade of staging. An example widely studied is the formation of Cu_xTiS_2 with the presence of the liquid electrolyte $\text{CH}_3\text{CN}/\text{CuCl}$ ⁵.

3.3.4. Rate Enhancement methods

Intercalation reactions often require a large period of time and elevated temperatures, later in this research we will see the intercalation processes unfold along eight weeks. Because of these time problems, rate enhancement methods have been developed, decreasing the reaction times and allowing to work with lower reaction temperatures^{1,5}. The most disadvantage in front of the conventional methods it is the decrease of the final product crystallinity. In addition, it is found intercalation compounds by using microwave heating can be achieved quickly retaining the products crystallinity. In addition, the ultrasonic irradiation of reactions mixtures increases the rates of intercalation of organic and organometallic compounds into MoO_3 , ZrS_2 and TaS_2 ⁵.

3.4. INTERCALATED 2D COMPOUNDS

The question is, why intercalated 2D compounds are scientifically important? This chapter exhibits the most relevant aspects about intercalated materials. After modifying a material chemically or physically new properties can be achieved. To begin, we can observe new electronic properties especially in the ultrathin region of single layer 2D nanomaterials because of the electron positioning¹. These characteristics are fundamental for the study of the electronic devices and condensed matter physics. Moreover, 2D nanomaterials presents an excellent mechanical strength, flexibility and optical transparency due to their atomic thickness and the strong bond between planes¹.

In view of the fact that ultrathin 2D nanomaterials presents special structural characteristics have been found a lot of applications^{1,6,7} such as electrocatalysis and photocatalysis, electronic/optoelectronic devices, batteries, supercapacitors, solar cells, biomedicine and

sensors, among others. There are various synthetic methods for preparing ultrathin 2D nanomaterials such as microchemical cleavage, mechanical force-assisted liquid exfoliation, ion intercalation assisted liquid exfoliation, oxidation-assisted liquid exfoliation and selective etching assisted liquid exfoliation, chemical vapor deposition (CVD) and molecular beam epitaxy (MBE).¹⁶⁻¹⁸ All of these synthetic methods can be categorized into two groups. The top-down methods include all the liquid exfoliation techniques commented, based on the exfoliation of the bulk material. The bottom-up ones are based on the layered growth, including the CVD and MBE techniques. At the present times, the development of these bottom-up methods are suitable to obtain all types of ultrathin 2D nanomaterials without being exfoliated. As commented previously, diverse exfoliation procedures have been developed¹. All top-down methods are based on the interlayer forces of two-dimensional compounds.

Mechanical exfoliation or microchemical cleavage (ME) is the simplest, fast and low-cost method based on weaken the *van der Waals* interactions without breaking the in-plane bonds. The most known procedure is the Scotch tape or *Nitto* tape^{16,19}, method that will be used on the experimental part of this investigation, and in the past, was used to obtain the first monolayer graphene³. ME have a lot of positive aspects such as keep the material integrity and high crystallinity due to no other substances are related during the process. Unfortunately, this method presents a disadvantage that limit his applications, the low efficiency and problems to transfer sample to substrates or devices. In principle, ME can be applied with all kind of 2D ultrathin nanomaterials^{1,18}. The Liquid-Phase exfoliation (LPE) process is another common method to obtain monolayer or few-layered materials. This method contains mechanical force-assisted liquid exfoliation, ion intercalation assisted liquid exfoliation, oxidation-assisted liquid exfoliation and selective etching assisted liquid exfoliation, ultrasonic exfoliation and liquid shearing methods. The LPE methods, on the contrary of ME methods, could achieve a higher efficiency but the problem to introduce solvent in the process.¹

The MBE is the bottom-up method par excellence based on the epitaxial growth²⁰. Due to the high cost of this technique, CVD is a good alternative. CVD is a traditional technique based on layered growth of the material and has been used on modern technologies for electronic devices. CVD is an interesting method to obtain ultrathin nanosheets of TMDs (e.g. MoS₂, MoSe₂, WS₂, etc.) and h-BN^{1,21}.

3.4.1. Transitional metal dichalcogenides

One of the most significant host lattice structures are the transition metal dichalcogenides (TMDs). These structures consist of two hexagonal lattices of chalcogen layers, and between these two layers the metal ions are placed. Metals in dichalcogenides can adopt an octahedral or trigonal prismatic symmetry. Within layers there is a mostly covalent/ionic bond and *van der Waals'* interactions appears between layers^{1,22}. Giving MoS₂ as an example and studying the intra- and inter- layer forces of dichalcogenides the infrared spectroscopy⁵ studies show that the interlayer interactions are 100 times weaker than the intralayer forces.

Most studied systems are those that insert lithium cations between the layers, mainly to the possibly battery applications^{1,3}. When the intercalation of an alkali metal ion is done, there are significant changes in the lattice parameters and alkali metals are ionized. Because of this, the intercalation complexes can adopt an extend variety of structures. Moreover, Lewis base organic molecules like ammonia, pyridine and alkylamines, can be intercalated into metal dichalcogenides by direct reactions at high temperatures⁵. Furthermore, redox active organometallic compounds also can be intercalated by direct reaction, ion-exchange or electrochemical reactions⁵.

In parallel, after intercalation dichalcogenides undergo electronic properties changes supporting the fact there is a charge transfer from the intercalated guest to the host lattice. Not long ago, it was observed intercalated dichalcogenides present the phenome of superconductivity in which the superconducting critical temperature (T_c) is higher than in the opening host compound. Some cases of layered semiconductors that have been transformed to superconductors are known such as ZrSe₂, MoS₂ and SnSe₂⁵. What is more, it is possible to obtain 2D nanosheets of this type of materials by suppressing the bulk compound to a liquid-phase exfoliation, concretely the ultrasonic method or microchemical cleavage¹.

Table 4: Examples of metal dichalcogenides host lattices with different ion and molecules guests⁵

Host	Guests
TiS ₂	Li, K, Cs
TaS ₂	Na, NH ₃ , Pyridine, [Co(Cp) ₂], [Fe ₆ S ₈ (PEt ₃)]
ZrS ₂	[Mo(η -C ₆ H ₆) ₂], [Mo(η -C ₆ H ₃ Me ₃) ₂]
MoS ₂	Li, Rb

3.4.2. Transition metal oxyhalides

The next relevant host lattice structures are the metal oxyhalides with the general formula of MOX where X is the halogen and M can be Fe, Cr, V or Ti. The best known structure is the FeOCl type but metal oxyhalides also adopt structures such as InOX where X could be Cl, Br or I^{1,5}. FeOCl is more reactive than metal dichalcogenides due to its stronger oxidizing power. That is to say, much more of organic which are good electro donors, and organometallic compounds have been intercalated into these host lattices by direct reactions. Consequently, occurs the expansion of the unit cell and there is no more successive layers plane stacked. It is known that transition metal oxyhalides are paramagnetic semiconductors and after the guest intercalation, the electrical conductivity of the FeOCl lattice increase significantly⁵.

Table 5: Examples of intercalation compounds of MOCl⁵

Host	Guests
FeOCl	Li ⁺ , NH ₄ ⁺ , NH ₃ , Pyridine, Pyrrole, [THF] ⁺ , [Fe(Cp) ₂], [SnMe ₃ (C ₅ H ₄ N)]
VOCl	[Co(Cp) ₂], Pyridine
TiOCl	[Co(Cp) ₂]

3.4.3. Metal trichalcogenidophosphates

In other matters, the metal trichalcogenidophosphates are a class of inorganic compounds with the general formula MPS₃ where M is a divalent metal ion such as Mg, V, Mn, Fe, Co, Zn, Ni, Pd and Cd, based on a distorted CdCl₂ lattice type^{1,23}. Among all the metal trichalcogenidophosphates, the intercalation of Li into NiPS₃ has potential applications as a battery materials^{6,24}. However, the intercalation of alkali metal ions it has been less studied than into the metal dichalcogenides. Taking MnPS₃ as an example, it is the most reactive compound by intercalation ion-exchange without assistance. The intercalated metal trichalcogenidophosphates series present interesting magnetic behavior, but on the contrary, the electronic conductivity of the intercalates it is not modified⁵. After the intercalation process, it can be obtained 2D ultrathin monolayer or few-layered metal trichalcogenidophosphates with mechanical exfoliation¹.

Table 6: Examples of intercalates of Metal trichalcogenidophosphates⁵

Host	Guests
MnPS ₃	K, NMe ₄ , pyH, [Co(Cp) ₂]
CdPS ₃	K, [Co(Cp) ₂]
FePS ₃	Net ₄ , [Co(Cp) ₂]
NiPS ₃	[Co(Cp) ₂], Cu, Na

3.4.4. Metal oxides

The oxides of the transition metals in high oxidation states also presents a layered structure. Metal trioxides with general formula MO₃ where M is the transition metal form multiple covalent bonds to oxygen with *van der Waals'* gaps. For instance, MoO₃ contribute on topotactic redox chemistry¹. The most studied intercalation reaction is the insertion of hydrogen into molybdenum trioxide to form the *oxide bronzes* (H_{0.5}MoO₃)⁵. With LiBuⁿ, LiBH₄ or electrochemically the lithium intercalation is possible. Another remarkable transition metal trioxide is V₂O₅. Consist in a layered structure with strong interlayer interactions. Because of that, the intercalation is easily when the cation guest species are small such as H⁺ and Li⁺.⁵ The layered A_xMO₂ oxides consist of a layer of alkali metal ions (A) between MO₂ layers. Within metal-oxygen layers there is MO₆ octahedra sharing vertex with the inserted guest. Regarding to the electrical properties, all of these intercalation compounds present a high electrical conductivity^{25,26}. As described at the beginning of this section, exist diverse liquid exfoliation methods. Concretely, ion exchange-assisted liquid exfoliation is useful to obtain monolayers or few-layered metal oxides¹.

Table 7: Examples of intercalation compounds of metal oxides⁵

Host	Guests
MoO ₃	H ⁺ , NH ₃ , Li ⁺ , Py, [Co(Cp) ₂], NH ₄ ⁺
V ₂ O ₅	Li ⁺ , C ₆ H ₅ N

3.4.5. Graphite intercalation compounds

Carbon is one of the most remarkable of all chemical elements. The carbon materials have extended diversity of structures with different physics and chemical properties. Graphene is the basic structural element of other allotropes such as graphite, fullerene, carbon nanotubes,

graphyne and other related materials²⁷. For definition, graphene is a 2D allotrope of carbon that presents a hexagonal lattice. This structure consists of covalent bonds where each atom bonds to three neighboring atoms adopting a sp^2 hybridization. That is to say, graphene is a single layer of carbon atoms forming a 2D honeycomb lattice plane²⁸.

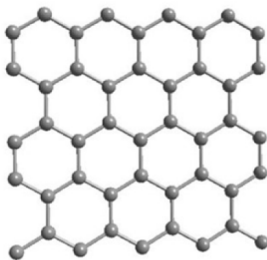


Figure 7: Graphene and graphite representation¹

Graphite is the thermodynamically most stable form of carbon at room temperature where the layers of graphene are stacked together by *van der Waals forces*. It is important to say that layers are displaced and for this reason, the center of hexagons lie above a carbon in the next layer (see Figure 1). GICs are complex materials that presents CX_m formula where X is the intercalated ion and m tend to be less than 1²⁹. These materials present a wide range of electrical and redox properties. Alkali metals GICs are the best-known donor type of graphite intercalation compounds because are easy to prepare such as C_8K . Also, can form intercalate compounds with electron acceptors, for instance, Br_2 , AsF_5 , HNO_3 and XeF_4 ⁵.

Carbon-based 2D nanomaterials have been deeply studied for Li-S batteries such as graphene because facilitate the intercalation/deintercalation of electrolyte ions, presents a high specific surface area, ultrahigh electrical conductivity and structural stability. Owing to the successful applications of graphene in Lithium-ion batteries (LIBs) it has been studied graphene analogous such as MoS_2 to explore the rechargeable batteries^{1,30,31}. However, graphene tends to aggregate and form graphitic structures. The aggregation of graphene causes a loss of unique properties, for example, high surface area and efficient mass transfer. In spite of aggregation, the research continues to develop graphene-based electrodes for supercapacitors. The first monolayer graphene was obtained by mechanical exfoliation^{1,16,19} but another common method such as liquid phase exfoliation is also useful to obtain nanosheets of graphite¹.

3.4.6. MXenes

MXenes are 2D layered transition metal carbides and/or nitrides with general formula $M_{n+1}AX_n$ where $n = 1, 2$ or 3 , M is the transition metal, A is an element from group III or IV and X can be a carbon or nitrogen. The adjacent layers are strongly bonded and consequently the exfoliation of this structure is different from graphite and TMDs where the layers are connected with *van der Waals* forces. The M - A layers presents a high reactivity. Therefore, is easily removed with the appropriate etching reagent without breaking the bonds in M - X layers and because of their interlayer spacing can undergo ion intercalation^{32,33}. As graphene, MXenes are 2D nanomaterials that have ultrahigh electrical mobility, and it has been explored as anodes for LIBs. When these layered transition metals work as supercapacitors electrodes guarantees high charge-transfer efficiency. MXenes have also been used for Li-S batteries^{1,30}. In addition, 2D ultrathin nano-MXenes can be obtained by ultrasonic exfoliation method as TMDs, covalent organic frameworks (COFs), graphene and h-BN¹.

In brief, after the intercalation process it has been achieved intercalated 2D materials with significantly changes related to the electronic and magnetic properties⁵. As we have been seeing in this chapter, most of the intercalation compounds suffer an increase of electrical conductivity. Indeed, 2D materials present catalytic applications due to the interesting structural and electronic properties such as the high surface-volume ratio¹. Applications of intercalates have been numerous and are emerging on the industrial level such as heterogeneous catalysis and energy storage with hosts that presents conductivity properties^{5,31}.

On laboratory scale, it has been developed new analytical techniques based on this phenome. Intercalation chemistry is an important discipline on the sphere solid state chemistry, material science, analytical, inorganic, organic and physical chemistry. At present times, the mechanistic details of intercalation chemistry it stills being studied to understand all aspects of intercalation systems¹⁴.

3.5. INTERCALATED IONIC ROCK-SALTS STRUCTURES

In this project, we will study the intercalation of Br_2 molecules into various metal halides to obtain layered ionic intercalation compounds for a subsequent study of the exfoliation properties and an analyze the possible 2D nanoflakes. This will open a completely new family of 2D materials containing only ionic intralayer bonds. The systems must present a rock salt structure with +1 and

-1 ions because of the interlayer interactions are not very strong and it is possible to intercalate halide molecules, i.e., Br₂. Chloride and fluoride of heavy alkali cations are the best options because of the large unit cell that allows to accommodate the bromine molecules while bromine systems result in non-desired trihalides structure and iodide systems are oxidized by bromine. The intercalation of bromine molecules transforms the cubic lattice of cesium fluoride into a layered structure. As a result, CsF·Br₂ structure can be described as a (Br-Br···F)_∞ chains and a tetragonal arrangement of cesium ions or CsF layers parallels to the ab plane with bromine molecules between layers parallels to the c axis. ³⁴⁻³⁶

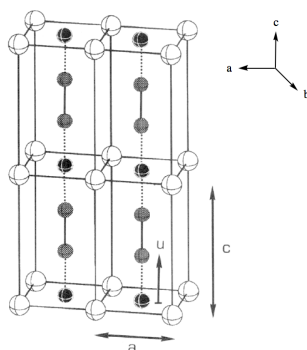


Figure 8: Crystal structure of CsF·Br₂. White, gray and black circles represent Cs, Br and F respectively. Reproduced with permission from ref³⁶

This section describes the predicted results of one of the most important metal halides, the cesium fluoride. This salt combines a large cation with a very small anion adopting an NaCl-type lattice. The investigations³⁴ found that CsF can absorb Br₂ and I₂ to form CsF·X₂ complexes with different level of staging. The CsF·Br₂ 1:1 is formed with an excess of halogen, in this case bromine. The cubic structure suffers an overture allowing the bromide molecules to positioned among the fluoride atoms maintaining Cs···F layers similar to the (100) planes in the NaCl-type lattice. Owing to the decrease of the coordination number both cesium and fluoride followed by an enhancement of the attractive forces, the Cs-F bond distances in the CsF·Br₂ system are shorter than in pure CsF. The cesium-fluoride layers are eclipsed where Cs⁺ is placed above another cesium ion, and the same with the fluoride anion given that interlayer distance is quite large. In view of this fact, the repulsive forces between must to be small. Furthermore, the bromine molecules are placed between fluoride atoms and a slightly bond length increase bromine-

bromine take place. In other words, there is a charge transfer among fluoride ion to Br_2 . Moreover, Br-F distance is longer than in BrF molecule.^{34,36}

In an energetic point of view CsF can be considered a 2D structure. On the intercalation process a loss of electrostatic energy is found but surprisingly it can be compensated by the interactions between the atoms of bromide and fluoride. The predicted structure³⁶ of $2\text{CsF}\cdot\text{Br}_2$ consist in two CsF consecutive layers without bromine molecules. The second bromine layer is empty. The cesium-fluoride layers are placed as in CsF pure where each of the cesium ion is above fluoride ion and vice-versa. As in $\text{CsF}\cdot\text{Br}_2$ there is a charge transfer because the Br-Br distance is slightly shorter³⁵. Regarding to the charge transfer from F^- to Br_2 , it has been observed that is the reason why the cesium ions remains almost fixed respect the bromine atoms. Previously on this experiment it was assumed that I_2 intercalation behavior was similar to the bromine. Nonetheless, immediately the following reactions occur where the major product is Cs_2I_8 and the Cl_2 molecules does not react with CsF ³⁵.



Equation 2: Behavior of cesium fluoride and iodine³⁵

In brief, the CsF lattice is energetically close to a 2D structure. The intercalation process occurs under certain conditions with large time reaction, and when there is not any chemical reaction. The cesium fluoride and graphite have some structural similarities. Both have a second stage compound^{35,36}, $2\text{CsF}\cdot\text{Br}_2$ and C_{16}Br_2 respectively.

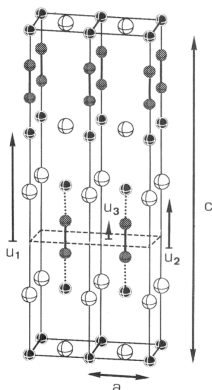


Figure 9: Crystal structure of $2\text{CsF}\cdot\text{Br}_2$. White, gray and black circles represent Cs, Br and F respectively.

Reproduced with permission from ref³⁶

To understand this energetical studies, the following figure illustrates all the structure variations and energetic contributions during the intercalation of bromine inside 3D metal halides.

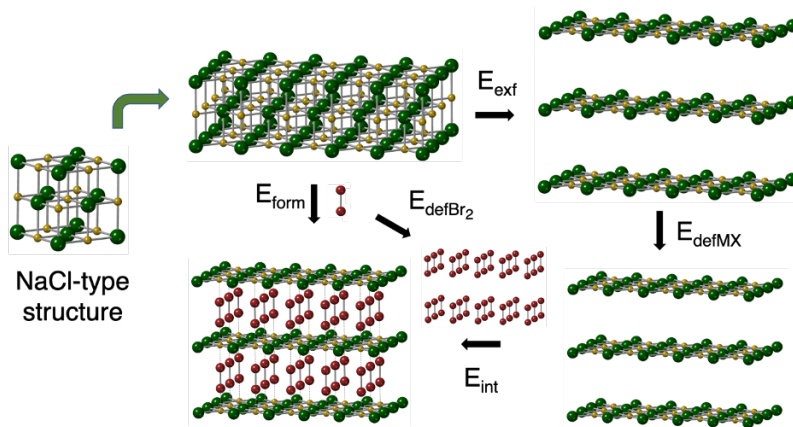


Figure 10: Energetic contribution in the intercalation bromine molecules inside 3D rock salt metal halides. The exfoliation energy (E_{exf}) to separate the MX layers and have more interlayer distance. The deformation energy (E_{defMX}) corresponds to the rearrangement of the 2D MX layer with the same M-X distances than in 3D structure. The interaction energy (E_{int}) corresponding to the energy between MX host and bromine molecules. The deformation energy of the Br₂ sublattice (E_{defBr_2}) is the necessary energy to change from the pure bromine molecule to the guest sublattice in the intercalation.

In this project we will focus on metal halides such as NaCl, KCl, NaF, KF, AgF and CsF which all adopt a NaCl-type lattice. Unpublished energy studies previously performed in the research group shows that the intercalation between Br₂ molecules and F⁻ is stronger than with Cl⁻, but surprisingly all the systems except NaF have negative formation energies (E_{form}) as shown on the Table 8. Moreover, the E_{int} and E_{form} defined on the Figure 10, indicate us the cesium fluoride is the best system to undergo an intercalation process followed by KF, KCl, AgF and NaCl. What is more, the E_{exf} of CsF system is an indicative sign that would be the easiest metal halide to exfoliate.

Table 8: DFT calculations by using the HSE06 functional (in kcal/mol) for the intercalation of Br₂ molecules inside NaCl-type 3D solids (MX·Br₂). Negative energy values indicate attractive interactions (E_{int}) or energetically favorable processes for the rest of energy values.

	CsF	KF	KCl	NaF	NaCl	AgF
E_{int}	-26.7	-22.4	-19.3	-15.2	-11.9	-25.0
E_{form}	-18.2	-7.9	-5.7	9.5	-0.4	-2.2
E_{exf}	9.4	11.6	13.5	10.8	11.9	15.0

4. OBJECTIVES

The aim of this project was to:

- Study the insertion of the intercalant guest, in this case, bromine molecules into 3D rock salts with powder and single-crystal X-ray diffraction.
- Search the best systems to carry out an efficient insertion of small molecules into metal halides.
- Study the exfoliation properties of intercalation compounds with the Atomic Force Microscopy.

5. EXPERIMENTAL SECTION

This project has been done in the Electronic Structure laboratories of the Inorganic and Organic Chemistry Department of the University of Barcelona. During the last decades, some effective characterizations techniques have been developed to establish the composition, size, thickness, crystallinity, defects, oxidation and electronic states of ultrathin 2D nanomaterials. The field of nanotechnology has experienced an important development, and nowadays with these new characterization techniques it is possible to detect the different structural characteristics of ultrathin 2D nanomaterials synthesized with diverse methods. Moreover, a clear characterization is important to understand the connection between structural characteristics and functionalities of nanomaterials. There are a large number of characterization techniques, for instance, optical microscopy, SPM, SEM, TEM/STEM and Raman spectroscopy among others¹. Due to the limitations of each technique, it is deeply recommended combine some techniques to have different perspective and end up understanding all the structural features and properties of 2D nanomaterials. This project is focused on the characterization with Atomic Force Microscopy and X-ray diffraction.

5.1. EXPERIMENTAL PROCEDURE

In order to obtain large crystals where bromine could be intercalated, it has been prepared saturated solutions of 3D rock salts with Mili-Q water and placed on the 316-steel tray to carry out the evaporation of the solvent. This tray was resistant to fluorides and chlorides, but for lack of time, only the NaCl and KCl were recrystallized. This process take place by the increase of the temperature with a water bath or leaving the solutions at room temperature several days.

Following the *Ephraim-Fajans* solubility rules^{37,38}, displays that the less soluble salts were those that contains a similar radium of cations and anions. Due to the major size of the Cl⁻, the 3D rock salts containing chloride as anion was expected to present a low solubility than fluoride salts (see table 9), obtaining large crystals. Therefore, it can be predicted cesium fluoride will be the most soluble salt because of the close ionic radium values.

Table 9: Solubilities of chloride halides at 20°C

	Solubilities (g/100 mL H₂O) at 20°C
NaCl	36.6
KCl	34.4
NaF	0.042
KF	102
AgF	210.6
CsF	367

Moreover, about chloride and fluoride halides which for lack of time could not be recrystallized, melting process was employed. The melting method consist of one hour and half heating ramp up to the melting point of the metal halide. When the metal was melted, it is applied another decreasing temperature time. The fluorides tend to be hygroscopic, in this case the cesium fluoride is the most problematic one. In order to avoid this problem, a short time must pass between taking out the melted metal halide and poured on a steel surface under nitrogen atmosphere.

Table 10: Melting points of all studies metal halides

Metal halide	Melting point (°C)
NaCl	803
KCl	771.5
NaF	993
KF	856
AgF	433
CsF	705

The following step was to intercalate the Br₂. The general procedure for the preparation the glass tubes that contains the mixture of metal halide previously recrystallized or melted, and bromine

started by adding around 0.5 g of metal halide and an excess of Br₂ in a dried glass tube. Once the mixture was cooled, it was started with the sealing method. With the hydrogen flame the glass tube was melted without completely sealing it. The tub was cooled again with ice and NaCl, and straightaway vacuum was applied. To conclude the sealing procedure makes use of a blowtorch. The resulting sealed tub was settled at room temperature and it was placed inside a glass recipient. Afterwards the tub has been left at the heater under 75°C for one, four and eight weeks (see Appendix 1 for times reactions) ready for being exfoliated.

5.1.1. Exfoliation method and preparation of the sample for the AFM

All-dry viscoelastic stamping method has significant advantages over other methods with some wet-chemical steps (see Section 3.4.). The flake 2D crystals were deposited into Si₃N₄ wafer by mechanical exfoliation with *Nitto* tape^{16,19}. A small portion of the sample was placed on the sticky part of the tape to achieve nanoflakes. The transfer was based on the viscoelasticity by slowly peeling off the sample. When it comes to transfer the nanoflakes to the Si₃N₄ substrate, this acceptor surface was placed into the *Nitto* tape where there was less sample in order to complete the flake transference for a later AFM analysis. The method is useful for any type of layered crystal but presents a poor effectivity. A remarkable aspect is that if an excessive pressure was applied while the transfer operation the viscoelastic part of the *Nitto* tape also will be transferred.

After analyzing all the samples previously exfoliated with the method that being said, we realized it could not be assumed the AFM images belong to exclusively the sample transferred because the AFM analyze has been showed very regular nanoflakes about 5nm. Afterwards, it was found the Si₃N₄ surface present scales of 5nm thickness and this is the reason why we could not guarantee that AFM images have been belong to the studied samples. Due to the added difficulties, another method was used. This new mechanical exfoliation technique was based on a thin layer of transparent elastomer called Polydimethylsiloxane (PDMS)^{39,40}. Bulk layered crystal of intercalated alkali halide is efficiently exfoliated using another *Nitto* tape less sticky to obtain a better sample transfer. Straightaway, a thin film of PDMS, previously adhered to a glass slide gets in touch with the exfoliated sample. The surface of the stamp was inspected under optical microscope to confirm the presence of flakes. In order to transfer sample flakes to the Si₃N₄ wafer, the stamp was pressed against the Si₃N₄ surface and was suppressed under 75°C about 15

minutes. The nanoflakes of interest were selected for their aspect because tend to have a different and variable coloration, as function of their width, compared to the other flakes of sample. Once thinner flakes were selected, the samples were ready to be analyzed by AFM.

5.1.1.1. Other tests performed

An alternative method to transfer the sample effectively into the acceptor surface was related to the PDMS solubility with organic solvents. The propose of this experimental procedure was to eliminate the elastomer film leaving the sample flakes into the acceptor surface. After putting in contact the Si_3N_4 wafer with PDMS surface containing the transferred flakes, it was searched for non-polar organic solvents in order to dissolve it. Due to the low polarity of the elastomer, it was tried with cyclohexane, toluene and acetone^{39,40}. The experimental results show that acetone was the best option because when Polydimethylsiloxane was exposed on this solvent lose its properties and dissolves. It is important not to leave too much acetone on the surface acceptor to avoid experimental complications on the AFM analysis, but apparently, the thermal method previously mentioned seems to be the most effective transferring method. In order to improve the sample transfer, the silicon Si_3N_4 support was replaced by silicon oxide support because of their ionic character.

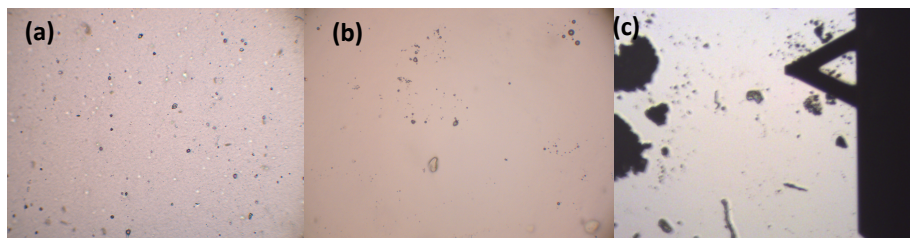


Figure 11: optical microscopy and AFM images of exfoliation flakes into (a) *Nitto* tape (b) PDMS (c) SiO_2 support

5.2. POWDER X-RAY DIFFRACTION

Powder X-Ray diffraction was performed with a PANalytical X'Pert PRO MPD alpha1 powder diffractometer in a Bragg-Brentano $\theta/2\theta$ of 240 millimeters of radius, in a variable automatic divergence split to get an illuminated length in the beam direction of 10 millimeters. It has been used $\text{Cu K}\alpha_1$ radiation ($\lambda = 1.5406 \text{ \AA}$) and a Ge (1 1 1) primary monochromator. The samples have been measured twice, immediately after prepared standard fast $\theta/2\theta$ scans from 4 to 100°

2θ with step size of 0.026° and a measuring time of 100 seconds and also, with a full range $\theta/2\theta$ statistics scans from 4 to $145^\circ 2\theta$ with step size of 0.013° and a measuring time of 200 seconds.

5.3. ATOMIC FORCE MICROSCOPY

Atomic Force Microscopy (AFM) is a useful tool that enables to explore, visualize and to perform measurements of sample thickness of 2D flakes. This method has been combined with some other techniques, in our case, powder and single-crystal XRD. The characterization of 2D flakes can be done with AFM, so it is important to remark characteristics about how an Atomic Force Microscopy works. Mainly, this type of microscope operates by scanning an AFM probe across a sample surface. An AFM has a Z scanner that moves the cantilever up and down and XY scanner that moves the sample back and forth underneath the cantilever to achieve a surface image in 3D. The probe contains a tip of four or five μm at the end of the cantilever which is typically 100-200 μm long, placed on a holder chip. When AFM starts to operate, the atoms of the tip interact with the surface of the sample by intermolecular forces and the cantilever is deflected. This technique uses a laser beam deflection system where the laser is reflected from the back of a cantilever onto a photodiode. The detector AFM generates an accurate topographic map of the surface using a feedback loop to control the height of the tip above the surfaces. What is more, this instrument presents different operation modes based on the interactions between the tip and the sample surface^{1,41,42}.

The contact mode applies a constant repulsive force between the sample and the tip. The advantage of this operation mode is the simplicity of its technology. Nonetheless, this contact can damage the sample and grind down the sharp tip, decreasing the quality of the image. An alternative operation is the tapping mode or dynamic mode where the cantilever oscillates swiftly up and down closer to the sample than the non-contact mode. While the cantilever moves vertically, the laser beam deflects over a photodiode array generating a sinusoidal electronic signal. The reflected laser beam informs about the vertical height of the sample. Finally, the non-contact mode uses an attractive force in the distance of the sample. As well, it is a dynamic mode where the probe oscillates not very close to the surface of the sample, leaving the surface untouched⁴¹.

In this research, it will be used the mode ScanAsyst, which is very similar to the tapping mode, the most productive way to use AFM to quickly capture a high-quality image⁴¹. This mode of operation is based on a new imaging mode called Peak Force Tapping. In contrast to the tapping mode,

ScanAsyst supply a direct force control increasing the resolution by managing the force that the tip applies to the sample and decreasing the contact area between both. What is more, the deformation and lateral forces are minimal and consequently the sample is not damaged. Moreover, ScanAsyst auto-optimize the scanning parameters like setpoint and scan rate.

Non-contact AFM has many advantages over contact AFM. It conserves the sample because the tip and the surface sample are not touching. This is the reason why with non-contact mode the lifetime and sharpness of the tip it is longer obtaining high quality imaging over many scans. This is a very important plus advantage because the tips are expensive to replace^{41,42}.

6. RESULTS AND DISCUSSION

6.1. INTERCALATION OF Br_2 IN NaCl-TYPE METAL HALIDES

An important sign to know about the efficiency of the intercalation reaction is the color adopted for the samples because all the halides and also the equivalent alkali bromides are white with the exception of the silver. If we compare each metal halide that has been in contact with bromine one, four and eight weeks, it can be seen differences on the coloring due to the bromine orange-red coloration. We can consider that the most colored sample has experienced a more effective intercalation process. Furthermore, when the AgF was melted, a powder grey solid was obtained. Due the coloration of the solid, it could be considered the oxidation of the silver. Because of this, instead of using the melted solid, only on this case the pure silver fluoride was employed to carry out the bromine intercalation process.



Figure 12: Differences on the coloring of the (a) $\text{CsF}\cdot\text{Br}_2$ systems (b) $\text{NaCl}\cdot\text{Br}_2$ systems (c) $\text{KCl}\cdot\text{Br}_2$ systems and (d) melted AgF

6. 2. X-RAY DIFFRACTION RESULTS

Powder X-Ray diffraction (XDR) allows to obtain structural information of the samples without having a suitable monocrystal sample. After analyzing the obtained diffractograms we realized the cesium fluoride X-ray results of four and eight weeks systems seems more similar to CsBr diffractogram than the intercalation CsF·Br₂ systems. Furthermore, hygroscopicity problems makes that the diffractogram of one-week CsF was of bad quality. The samples with 4 and 8 weeks are considerably less hygroscopic, thus, more stable in air. The main problem was the grinding of the samples before the diffraction and a loss of the intercalated bromine in such process. Thus, the final detected product in the diffraction was CsBr, that is white as CsF in contrast with the initial state of the brominated samples (see Figure 12). Thus, this technique as it was employed is not really useful to characterize the intercalated materials and single-crystal could be an alternative. (see Appendix 2 for all the cesium fluoride systems XDR diffractograms)

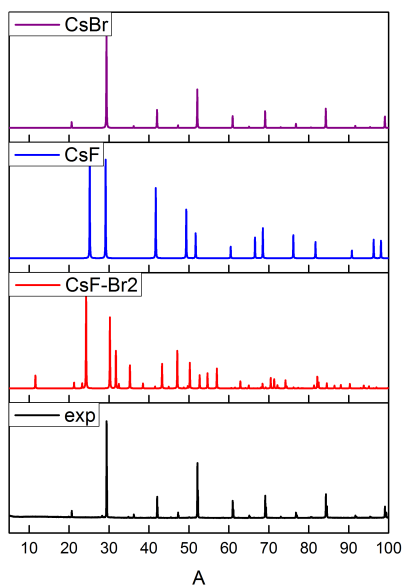


Figure 13: predicted comparative diagram between CsF, CsBr and intercalated CsF·Br₂ systems

6.3. CRYSTALLINITY

In front of the problems of powder XDR, the goal was to obtain a useful information and corroborate if the problem was the grinding process. Single-crystal X-ray diffraction of samples with reaction time of eight weeks were done. Firstly, it had to examine the systems to determine if there were monocrystals. The NaCl, KCl, CsF, NaF, KF and AgF systems, both melted and recrystallized were inspected with Greenough compact stereomicroscope which presents an apochromatic optical. Although all the inspected samples present polycrystallinity, it was found that probably only recrystallized NaCl and KCl systems could be suitable to suppress under monocrystal X-ray diffraction after select the most crystalline part of these two compounds. Regrettably, because of the polycrystallinity of the cesium fluoride samples and their powder aspect, it was not possible to be employed by single-crystal XDR. Probably, the reason is a loss of crystallinity because it is the most efficient system for the bromine intercalation.

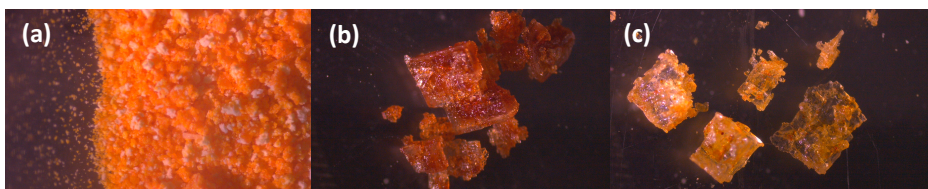


Figure 14: High resolution Stemi 508 images of the polycrystalline eight weeks samples (a) CsF (b) NaCl (c) KCl. It can be seen the two different type of samples contained in the cesium fluoride, the orange part is the intercalated one and the pallid part presumably is the initial CsF.

The parameters cell obtained displays in both, angles of 90° forming a trigonal structure. Due to the small values of the parameters a, b and c it could be assumed the intercalation process were not successful. The following step would be to try to obtain more crystalline samples to perform a complete monocrystal X-Ray diffraction, but for lack of time it has not been possible. (see Appendix 3 for the obtained parameters cell)

6.4. EXFOLIATION PROPERTIES

The goal of this section is the exfoliation and the transference of the sample flakes on the silicon wafer. However, the AFM analyze made us to doubt about the effectivity of the used methods because the images has been showed too regular flakes. After studying all the possibilities, it was found the Si_3N_4 wafer present scales of 5 nm thickness, exact flake width obtained during the AFM analysis. This is the reason why we could not guarantee that AFM images have been belong to the studied samples or to the silicon wafer. The PDMS method with

the SiO_2 support described at the experimental section was useful, allowing us to observe the nanoflakes on the AFM images (see Section 5.1.1.). Focusing with cesium fluoride, the eight weeks system present nanoflakes around 250 nm width. These positive results made us to continue the analysis with the four weeks samples, however, 300 nm nanoflakes were found indicating a smaller degree of intercalation. Due to the high hygroscopic character of the CsF it was impossible to exfoliate the one-week sample. The thickness about 200-300 nm indicates there were various nanoflakes placed together, therefore, the AFM analysis were focused on various eight-week systems in order to achieve a thinner nanoflakes, and finally, a flake around of 70 nm width was found. In the future, to obtain better results it could be performed a sonification process which is a liquid exfoliation method commented on the 3.4. section. (see Appendix 4 for the corresponding graphics)

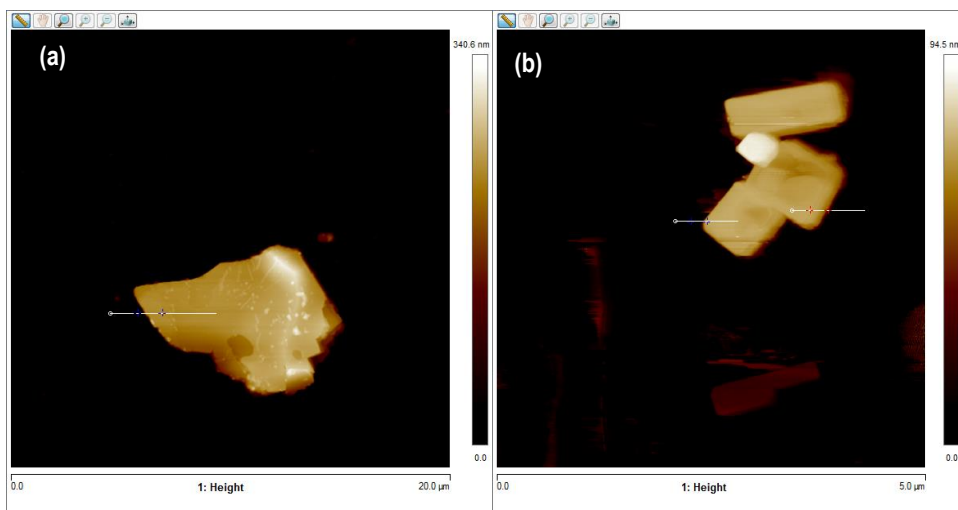


Figure 15: AFM high quality images of nanoflakes obtained (a) 250 nm flake of four weeks $\text{CsF}\cdot\text{Br}_2$ (b) 70 nm flake of eight weeks $\text{CsF}\cdot\text{Br}_2$

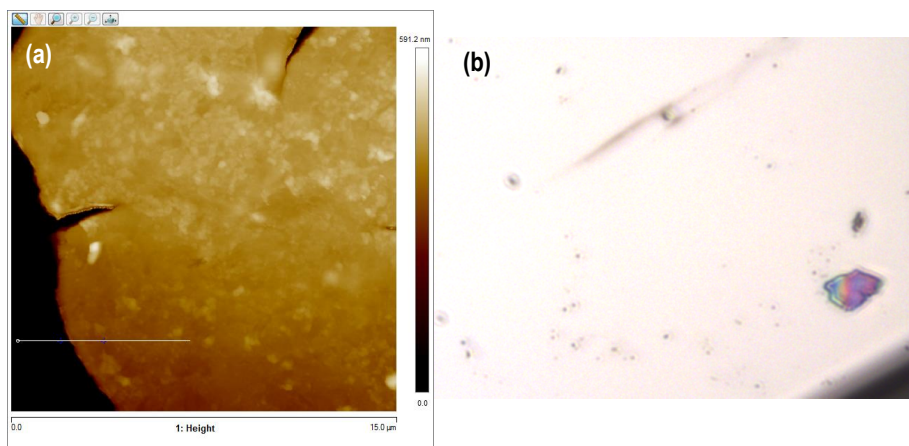


Figure 16: (a) AFM high quality image of eight weeks CsF·Br₂ nanoflake (300 nm) (b) AFM image of the colored 300 nm nanoflake.

10. CONCLUSIONS

- It can be considered partly of the obtention of ionic 2D systems were achieved, more in particular, the cesium fluoride systems. This fact could be assumed because of the coloration adopted and the decreasing of the hygroscopic character on the reaction times products of four and eight weeks systems. However, with the other studied systems we do not see such obvious results. In particular, with the AgF experimental complications were appeared. After the melting process it was obtained a powder gray solid instead of AgF melted crystals, indicative of the silver oxidation. This is because pure AgF was used as a reactant for the intercalation process.
- X-ray powdered diffractograms were not successfully obtained because of the previous grinding process of the samples which cause the loss of Br₂ obtaining the MBr species.
- X-ray single-crystal diffraction shows compounds with cells not easily recognizable apparently without intercalation. The systems with a successfully intercalation are not crystalline making impossible its analysis with single-crystal XDR.
- At the beginning, the study of cesium fluoride systems exfoliation properties were done with *Nitto* tape exfoliation followed by the transference of the obtained flakes into a Si₃N₄ wafer. Due to the low efficiency of this procedure, another method was tried successfully. The exfoliation of the samples also was done with *Nitto* tape but during the transference process the PDMS, a SiO₂ wafer and an increase of the temperature were involved. Positive results were achieved with a 70 nm width nanoflake.

11. REFERENCES AND NOTES

1. Tan, C. *et al.*; Recent Advances in Ultrathin Two-Dimensional Nanomaterials. *Chemical Reviews* **2017**, *117*, 6225-6331.
2. Trushin, M. & Schliemann, J.; Polarization-sensitive absorption of THz radiation by interacting electrons in chirally stacked multilayer graphene. *New J. Phys.* **2012**, *14*, 1-10.
3. Inamuddin, R. B., Ahamed, M. I., Asiri, A. M.; *Layered 2D Advanced Materials and Their Allied Applications*; 1st ed.; Wiley; **2020**, 1-382.
4. Guo, H. W., Hu, Z., Liu, Z. B. & Tian, J. G.; Stacking of 2D Materials. *Advanced Functional Materials* **2021**, *31*, 4891-4903.
5. Averill, B. A.; Inorganic materials edited by D. W. Bruce and D. O'Hare. *J. Appl. Crystallogr.* 5th ed.; Wiley; **1993**, *26*, 165-228.
6. Glavin, N. R. *et al.*; Emerging Applications of Elemental 2D Materials. *Advanced Materials* **2020**, *32*, 1-69.
7. Cheng, J., Wang, C., Zou, X. & Liao, L.; Recent Advances in Optoelectronic Devices Based on 2D Materials and Their Heterostructures. *Advanced Optical Materials* **2019**, *7*.
8. Chaves, A. *et al.*; Bandgap engineering of two-dimensional semiconductor materials. *npj 2D Materials and Applications* **2021**, *4* 1-21.
9. Li, Y.; 2D Inorganic Materials: from Atomic Crystals to Molecular Crystals. *Chemical Research in Chinese Universities* **2020**, *36*, 147-148.
10. Yazzev, O. V & Kis, A.; MoS₂ and semiconductors in the flatland. in *Materials Today* **2015**, *18*, 20-30.
11. Jung, Y., Ji, E., Capasso, A. & Lee, G. H.; Recent progresses in the growth of two-dimensional transition metal dichalcogenides. *Journal of the Korean Ceramic Society* **2019**, *56*, 1-14.
12. Thakar, K. & Lodha, S.; Optoelectronic and photonic devices based on transition metal dichalcogenides. *Mater. Res. Express* **2019**, *7*, 1-25.
13. Gutiérrez, H. R.; Two-Dimensional Layered Materials Offering Expanded Applications in Flatland. *ACS Applied Nano Materials* **2020**, *3*, 6134-6139.
14. Zhou, X. *et al.*; Intercalation of Two-dimensional Layered Materials. *Chemical Research in Chinese Universities* **2020**, *36*, 584-596.
15. Chen, Y. *et al.*; Two-Dimensional Metal Nanomaterials: Synthesis, Properties, and Applications. *Chemical Reviews* **2018**, *118*, 6409-6455.
16. Tao, H. *et al.*; Scalable exfoliation and dispersion of two-dimensional materials-an update. *Physical Chemistry Chemical Physics* **2017**, *19*, 921-960.
17. Tiwari, S. K., Sahoo, S., Wang, N. & Huczko, A.; Graphene research and their outputs: Status and prospect. *Journal of Science: Advanced Materials and Devices* **2020**, *5*, 10-29.
18. Le, T. H., Oh, Y., Kim, H. & Yoon, H.; Exfoliation of 2D Materials for Energy and Environmental Applications. *Chemistry - A European Journal* **2020**, *26*, 6360-6401.
19. Castellanos-Gomez, A. *et al.*; Deterministic transfer of two-dimensional materials by all-dry viscoelastic stamping. *2D Mater.* **2014**, *1*, 1-8.
20. Ginley, T. P., Wang, Y. & Law, S.; Topological insulator film growth by molecular beam epitaxy: A review. *Crystals* **2016**, *6*, 1-26.
21. Manawi, Y. M., Ihsanullah, Samara, A., Al-Ansari, T. & Atieh, M. A.; A review of carbon nanomaterials' synthesis via the chemical vapor deposition (CVD) method. *Materials* **2018**, *11*, 1-

- 36.
22. Fu, Q. *et al.*; 2D Transition Metal Dichalcogenides: Design, Modulation, and Challenges in Electrocatalysis. *Advanced Materials* **2021**, 33, 1-24.
23. Taylor, B. E., Steger, J. & Wold, A.; Preparation and properties of some transition metal phosphorus trisulfide compounds. *J. Solid State Chem.* **1973**, 7, 461-467.
24. Wang, C. *et al.*; Layered materials for supercapacitors and batteries: Applications and challenges. *Progress in Materials Science* **2021**, 118, 1-56 .
25. Védrine, J. C.; Heterogeneous catalysis on metal oxides. *Catalysts* **2017**, 7, 1-25 .
26. Chavali, M. S. & Nikolova, M. P.; Metal oxide nanoparticles and their applications in nanotechnology. *SN Applied Sciences* **2019**, 1, 1-30.
27. Yasuda, E. *et al.*; Carbon Alloys-Multi-functionalization. *Mater. Sci. Eng. B Solid-State Mater. Adv. Technol.* **2008**, 148, 7-12.
28. Jorio, A., Soares, E. A., Paniago, R., Rocca, M. & Vattuone, L.; Graphene. *Springer Handbooks* **2020**, 1171-1198.
29. Enoki, T., Endo, M. & Suzuki, M.; *Graphite Intercalation Compounds and Applications. Graphite Intercalation Compounds and Applications* [Online] **2003**, <https://oxford.universitypressscholarship.com/view/10.1093/oso/9780195128277.001.0001/isbn-9780195128277-book-part-4> (accessed March 5, 2021).
30. Shi, L. & Zhao, T.; Recent advances in inorganic 2D materials and their applications in lithium and sodium batteries. *Journal of Materials Chemistry A* **2017**, 5, 3735-3758.
31. Xu, J. *et al.*; Recent Progress in Graphite Intercalation Compounds for Rechargeable Metal (Li, Na, K, Al)-Ion Batteries. *Advanced Science* **2017**, 4, 1-14.
32. Naguib, M., Mochalin, V. N., Barsoum, M. W. & Gogotsi, Y.; 25th anniversary article: MXenes: A new family of two-dimensional materials. *Adv. Mater.* **2014**, 26, 992-1005.
33. Ronchi, R. M., Arantes, J. T. & Santos, S. F.; Synthesis, structure, properties and applications of MXenes: Current status and perspectives. *Ceramics International* **2019**, 45, 18167- 18188.
34. DesMarteau, D. D., Grelbig, T., Hwang, S. -H & Seppelt, K.; CsF·Br₂, an Alkali-Metal Halide Intercalation Compound. *Angew. Chemie Int. Ed. English* **1990**, 29, 1448-1449.
35. Drews, T., Marx, R. & Seppelt, K.; Cesium fluoride - Bromine intercalation compounds. *Chem. - A Eur. J.* **1996**, 2, 1303-1307.
36. Ruiz, E. & Alvarez, S.; Intercalation of Halogen Molecules in Alkali Fluoride Lattices: A Theoretical Study. *J. Am. Chem. Soc.* **1995**, 117, 2877-2883.
37. Hempstead, M. R.; Comparative inorganic chemistry. *Coord. Chem. Rev.* **1992**, 116, 269-270.
38. Morris, D. F. C.; Ionic radii and enthalpies of hydration of ions. *Structure and Bonding* **2008**, 116, 63-82.
39. Adamiak, W., Kaluza, D. & Jönsson-Niedziolka, M.; Compatibility of organic solvents for electrochemical measurements in PDMS-based microfluidic devices. *Microfluid. Nanofluidics* **2016**, 20, 1-7.
40. Lee, J. N., Park, C. & Whitesides, G. M.; Solvent Compatibility of Poly(dimethylsiloxane)-Based Microfluidic Devices. *Anal. Chem.* **2003**, 75, 6544-6554.
41. Butt, H. J., Cappella, B. & Kapp, M.; Force measurements with the atomic force microscope: Technique, interpretation and applications. *Surface Science Reports* **2005**, 59, 1-152.
42. Binnig, G., Quate, C. F. & Gerber, C.; Atomic force microscope. *Phys. Rev. Lett.* **1986**, 56, 930-933.

12. ACRONYMS

AFM – Atomic Force Microscopy

BP – Black Phosphorous

FA – Mamidinium

GICs – Graphite intercalation compounds

h-BN – Hexagonal Boron Nitride

LPE – Liquid-Phase exfoliation

LIBs – Lithium-ion batteries

MA – Methylammonium

ME – Mechanical exfoliation

PDMS – Polydimethylsiloxane

Py – Pyridine

TCPP – Tetrakis(4-carboxyphenyl)

TMDs – Transitional metal dichalcogenides

XDR – X-ray diffraction

APPENDICES

APPENDIX 1: TIMES OF EACH INTERCALATION PROCESS

Table 11: Studies metal halides and their times reactions

Metal Halide	weeks with Br ₂		
	1	4	8
KCl melted	16/03/2021	6/04/2021	4/05/2021
KCl recrystallized	30/03/2021	20/04/2021	18/05/2021
NaCl melted	19/03/2021	9/04/2021	7/05/2021
NaCl recrystallized	25/03/2021	15/04/2021	13/05/2021
KF	24/03/2021	14/04/2021	12/05/2021
NaF	30/03/2021	20/04/2021	18/05/2021
AgF	1/04/2021	22/04/2021	20/05/2021
CsF	23/04/2021	14/05/2021	–

APPENDIX 2: X-RAY POWDER DIFFRACTOGRAMS OF CsF

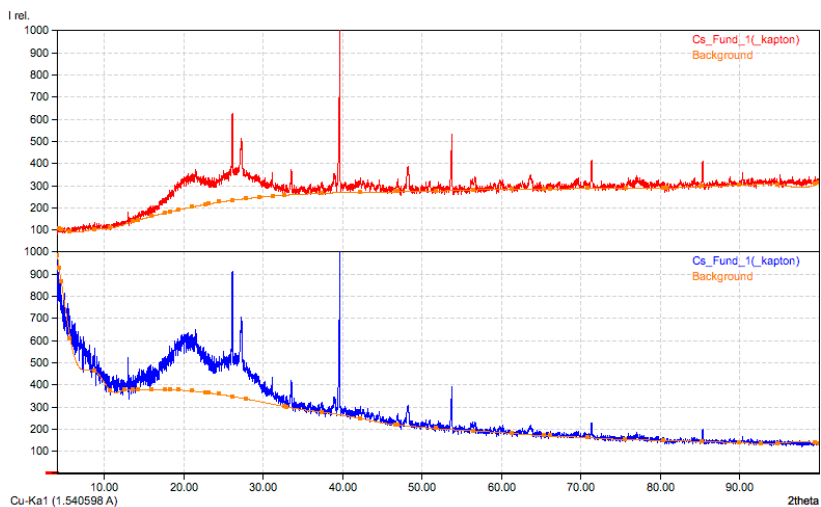


Figure 17: Powder XDR obtained for the CsF-Br₂ system of one week

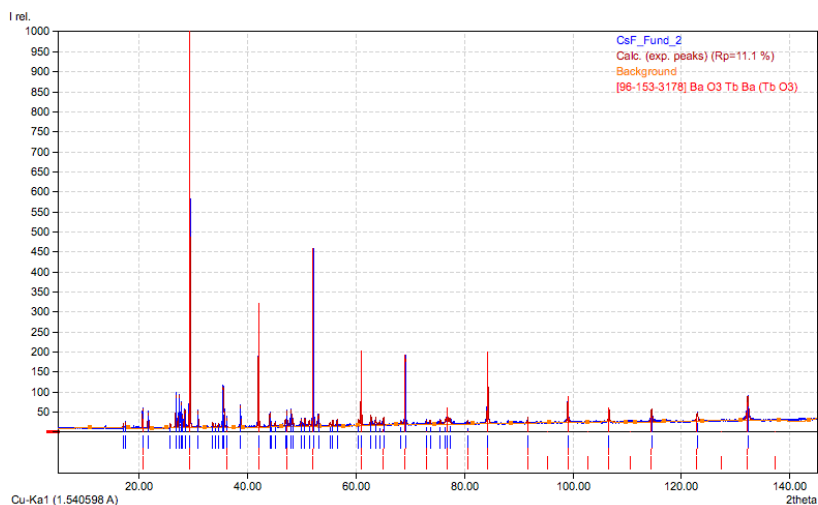


Figure 18: Powder XDR obtained for the CsF-Br₂ system of four weeks

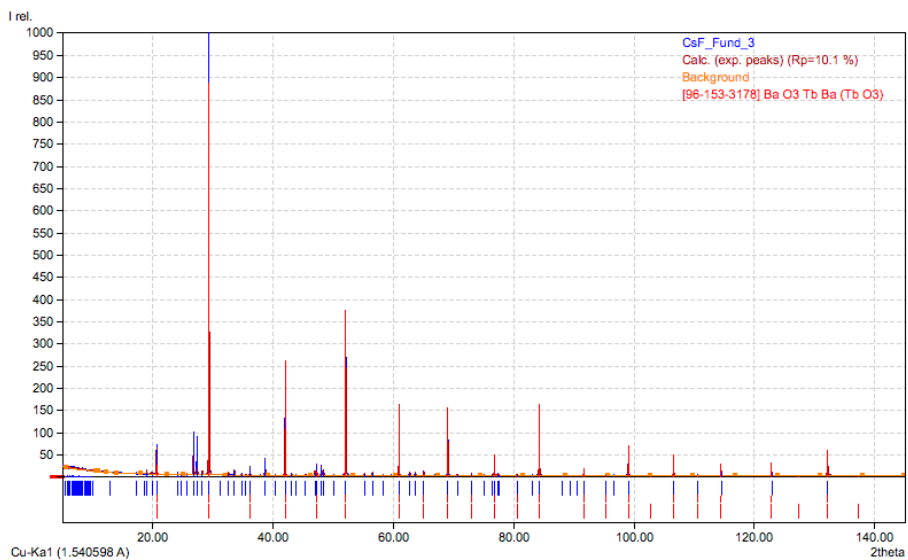


Figure 19: Powder XDR obtained for the CsF·Br₂ system of eight weeks

APPENDIX 3: X-RAY SINGLE-CRYSTAL RESULTS

Table 12: The parameters cell of NaCl and KCl crystals with only 24 images

NaCl				KCl			
a	3.77	α	60.69	a	4.27	α	60.69
b	3.81	β	60.80	b	4.37	β	61.64
c	3.86	γ	61.92	c	4.40	γ	61.03

APPENDIX 4: GRAPHICS OBTAINED WITH NANOSCOPE ANALYSIS PROGRAM

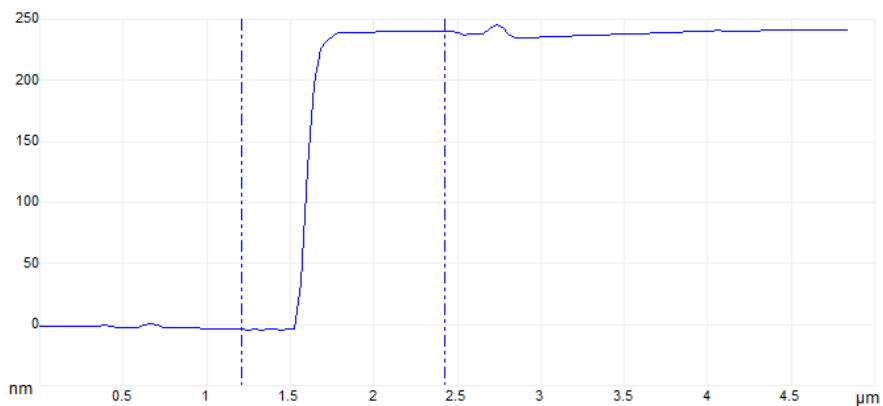


Figure 20: 250 nm nanoflake width along x-y

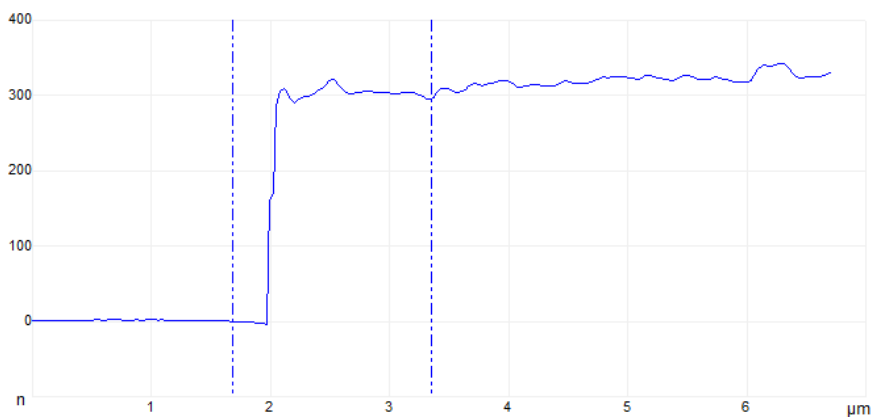


Figure 21: 300 nm nanoflake width along x-y

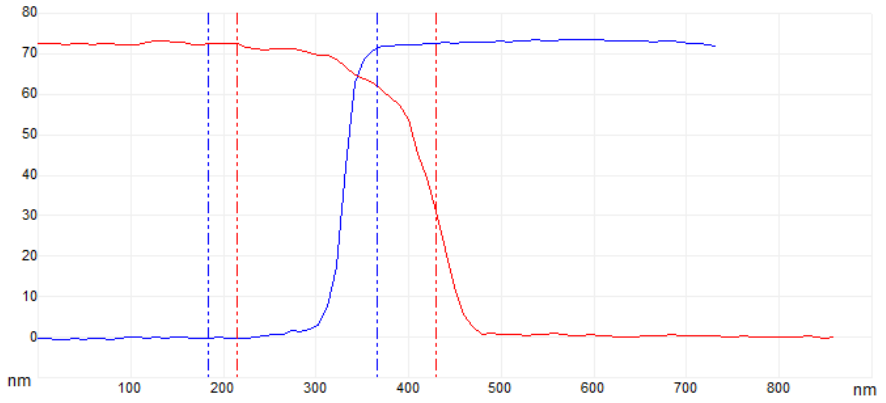


Figure 22: 70 nm nanoflake width along x-y

